



A Machine Learning Approach for Automated Detection and Classification of Cracks in Ancient Monuments using Image Processing Techniques

Ramani Perumal^{1,*}, Subbiah Bharathi Venkatachalam²

¹Assistant Professor, SRM Institute of Science and Technology, Ramapuram, Chennai-600089, India

²Director, SRM Institute of Science and Technology, Ramapuram, Chennai-600089, India

Emails: ramanip@srmist.edu.in; director@srmrmp.edu.in

Abstract

Stone monuments stand as enduring testaments to human history and cultural heritage, yet they are susceptible to deterioration over time. In this paper, we propose a comprehensive approach for the automated detection and classification of cracks in ancient monuments, integrating machine learning and advanced image processing techniques. Our method addresses the pressing need for efficient and objective assessment of structural integrity in these invaluable artifacts. The proposed algorithm begins with preprocessing steps, including image enhancement using adaptive histogram equalization to improve crack visibility. Subsequently, feature extraction techniques such as Grey Level Co-occurrence Matrix (GLCM) and Local Binary Pattern (LBP) are applied to capture essential characteristics of crack patterns. Central to our approach are the Back Propagation Neural Network (BPNN) and Improved Support Vector Machine (ISVM) classifiers, which are trained on the extracted features to detect and classify cracks with high accuracy. The BPNN learns complex relationships between input features and crack types, while the ISVM leverages a margin-based approach for robust classification. Through extensive experimentation on a diverse dataset of ancient monuments, we demonstrate the effectiveness of our approach in accurately identifying and categorizing cracks. The proposed method offers a scalable and objective solution for monitoring the structural health of ancient monuments, contributing to proactive conservation efforts and the preservation of cultural heritage.

Keywords: Stone monuments; Back Propagation Neural Network (BPNN) and Improved Support Vector Machine (ISVM); Grey Level Co-occurrence Matrix (GLCM); Machine Learning

1. Introduction

The responsibility of maintaining ancient structures and cultural artefacts is vital in the contemporary society we now inhabit. The maintenance of the infrastructure is the bulk of the Ancient Monument protection system. The project to maintain the Ancient Monument will need a number of different pieces of infrastructure, including the design and construction of the Ancient Monument and the development of the linkages in the Ancient Monument preservation junction. Improvements in the field of historic monument preservation are enabling it to grow into the community's rural and inland areas. The preservation of historic sites is directly responsible for this development. The Ancient Monument's care is within the purview of the preservation system's maintenance component. This part of the Ancient Monument's preservation method is essential. The air and floods that occur throughout the rainy season have caused cracks to form all over the Ancient Monument. The monument has been severely damaged as a result. In doing so, they cause breaches in the Ancient Monument, which eventually lead to its complete destruction. Cracks like this should be examined often to ensure that no precious ancient artefacts are lost, and it is crucial that the quality of the Ancient Monument be maintained to avoid the emergence of such faults in the Ancient Monument. Keeping the Ancient Monument in good condition is crucial if we want to avoid similar problems from developing in the future.

Over the course of this study, we were able to effectively identify problems in the preservation of historic sites by using Neural Networks (NN) and Support Vector Machines (SVM) as a classification approach. Several steps, such as preprocessing, the Gabor transform, feature extraction, classification, and segmentation, are rolled into the proposed technique. During the preprocessing phase, an adaptive histogram equalization approach is employed to improve the overall image quality of the Ancient Monument. This method improves the image of the Ancient Monument so that faults may be found in the construction more quickly and precisely, regardless of the ambient conditions. After the image has been preprocessed in the spatial domain, a multi-resolution version of the image is created by applying the Gabor transform to the image. These graphic displays, at many scales, information on the frequency, time, and direction of an event. The textural features of the multi-resolution image processed via Gabor are also available. Grey level co-occurrence matrices (GLCMs) and local binary patterns (LBPs) are two names for the texture characteristics we're interested in (LBP). Crack photographs and crack-free images may be distinguished from one another with the help of these distinguishing features, which highlight the differences between the two kinds of images. A neural network classifier (NN) and a support vector machine classifier (SVM) are now being trained and classified using the data collected from the features. Based on the feature set, these classifiers will decide whether or not the fractures are present in the image of the Ancient Monument. The last step involves performing morphological operations on the crack image in order to discover and isolate the fractures in the photograph of the antique classified monument. The cracked picture is processed in this way.



Figure. 1. Ancient Monument Images (a) Normal (b) with Cracks

As a result of the wear and tear from things like wind, water, and noise, cracks have emerged all throughout the framework of the Ancient Monument. The locomotive passes through a break in the crack, eroding a section of the Old Monument and making it seem less genuine. To assess the forms that weathering has taken on cultural heritage structures and the extent of their deterioration, scientific treatments are required. In addition, these actions contribute significantly to preservation and restoration strategies. These kind of interventions need to be nondestructive, on-site, rapid, efficient, and economical, with a graphical map indicating the location and amount of the damage [3].

Preserving ancient structures and cultural artifacts is paramount for maintaining our collective heritage and understanding of the past. However, the ongoing decay and deterioration of these historic monument's present significant challenges to conservation efforts. While manual inspection methods have traditionally been employed to assess the condition of these structures, they are often labor-intensive, subjective, and prone to human error.

In this study, we propose a novel approach for the automated detection and classification of cracks in ancient monuments. Given the complexity and variability of crack patterns in historical structures, we have chosen to leverage advanced machine learning techniques, specifically Neural Networks (NN) and Support Vector Machines (SVM), for crack detection and classification.

Neural Networks, particularly Back Propagation Neural Networks (BPNN), are well-suited for pattern recognition tasks and have demonstrated success in various image classification applications. By training a BPNN on a dataset of annotated images, we can develop a model capable of learning complex relationships between image features and crack presence, enabling accurate detection and classification.

Support Vector Machines (SVMs), on the other hand, are powerful classifiers known for their ability to handle high-dimensional data and nonlinear decision boundaries. By employing an SVM classifier, we can effectively separate cracked and uncracked images based on extracted image features, providing a reliable method for crack detection in ancient monuments.

Through the combination of these advanced machine learning techniques and image processing methods, we aim to develop a robust and accurate system for automated crack detection in historic buildings. By doing so, we hope to overcome the limitations of manual inspection methods and contribute to the preservation of our cultural heritage for future generations.

1.1 Stone Deterioration and Weathering Forms

Environmental variables like as storms, fires, high temperatures, rains, floods, and biological colonisation by creatures like fungus, algae, lichen, and moss may all contribute to the deterioration of stone buildings. [4] There is a wide range of manifestations that these environmental influences might take. There are many different kinds of weathering, including as natural, artificial, biological, chemical, and structural. The exposed object will be harmed by weathering, a natural process that takes place all year round and is affected by each of the four seasons. The effects of the elements, such as rain and wind, may cause monuments to peel, exfoliate, and disintegrate [5-9]. Deformed or cracked stones may have had their locations adjusted for structural reasons. Displacement is one possible result of this weathering [10]. The degradation of rock's chemical makeup is called "chemical weathering," and it is caused by various components dissolved in precipitation, surface water, or groundwater (such as sulphur, carbon dioxide, sulphur dioxide, nitrogen oxide, and nitric oxide). Yellow, brown, and white staining of the stone may come from chemicals reacting with water on the stone's surface [11, 13]. There is some evidence that manmade influences, such as dyes and paints, contribute to the deterioration of rocks. Weathering is an inevitable process that causes monuments to deteriorate over time. When analysing deterioration, one may use either a destructive or non-destructive method. There are benefits and drawbacks to both options. In disruptive research, materials were removed from their original context and analysed in a laboratory. Non-destructive testing is any approach used to examine or test a system's components that doesn't compromise their integrity or the part of the system being examined. Listed below are the specific steps involved in each of these processes. [14, 15].

1.2 Destructive Methods

Drilling Resistance: * A Quantitative Analysis In order to test the stone's durability, perforations are drilled into it. The material's reaction may tell you about its hardness and density. When there is a steady supply of energy and rotation, drilling is more efficient.

Scanning electron microscopy, or SEM for short. Repeatedly sending a beam of light back and forth creates images of a stone. It not only provides data for both micro and nanometric combinations, but also does analysis based on material composition [16].

X-ray diffraction analysis* (XDA) It is a reliable technique for identifying certain mineral components. Thin section microscopy is used in the inquiry to identify the various mineral components. This method may be useful for identifying clay minerals that have been modified by weathering agents, such as salts. Only a little sample of stone will do for this kind of study. Alteration or disintegration of minerals, the formation of new minerals, and their eventual dissolution are all effects of weathering.

1.3 Non-destructive Methods

The Use of an Eddy Current a magnetic field is created when an electric current flows through the coil, and an electric current is generated whenever the magnetic field changes. This field represents the conductivity attribute and is used to pinpoint the flaws. It is feasible to find flaws in the region when electromagnetic interference causes a measurable response. One major drawback is that this method can only be used to test conductive material.
*Testing with Ultrasound (UT)

The transducer is used to transmit the high-frequency signal to the rock. Defects in a material or part may be evaluated by measuring the amount of energy supplied and received. Its major function is to detect flaws under the surface of wood, polymers, and other materials; it can also assess thin portions, which are notoriously difficult to inspect (IRT) [17–23].

The infrared method is used to find out how the surface's temperature is spread. Not only is it useful for finding sources of heat, but it may also reveal faults, voids, and other geological discontinuities [24–26].

In response to these challenges, this study proposes a novel approach for the automated detection and classification of cracks in ancient monuments. By leveraging advanced image processing techniques and machine learning algorithms, we aim to enhance the efficiency and accuracy of crack detection, thereby facilitating more effective conservation efforts.

The significance of this research lies in its potential to revolutionize the way we assess and monitor the condition of ancient structures. By automating the process of crack detection, we can streamline conservation efforts, reduce the reliance on subjective human judgments, and ensure the timely identification of areas requiring intervention.

Furthermore, the proposed methodology has the potential to fill existing gaps in the field of heritage conservation. By combining machine learning algorithms such as Neural Networks and Support Vector Machines with image

processing techniques, we can develop a comprehensive system capable of accurately detecting and classifying cracks in ancient monuments. This not only enhances our ability to preserve these invaluable cultural artifacts but also contributes to the broader field of computer vision and pattern recognition.

For example, digital image processing is a non-destructive technology that may provide excellent results with little time and effort investment [27]. Because of this study, we now have a method for determining the kind of decay using a combination of Luminance and the Local Binary Pattern, as well as a novel decay assessment for quantifying the extent of decay.

Preserving ancient structures and cultural artifacts is paramount for maintaining our collective heritage and understanding of the past. However, the ongoing decay and deterioration of these historic monument's present significant challenges to conservation efforts. While manual inspection methods have traditionally been employed to assess the condition of these structures, they are often labor-intensive, subjective, and prone to human error.

This study seeks to address these challenges by proposing a novel approach for the automated detection and classification of cracks in ancient monuments. The main objective of the research is to develop a machine learning-based system capable of accurately identifying and categorizing cracks in photographs of historic buildings. By leveraging advanced image processing techniques and machine learning algorithms, we aim to enhance the efficiency and accuracy of crack detection, thereby facilitating more effective conservation efforts.

Specifically, this study aims to:

1. Develop a machine learning algorithm capable of detecting cracks in photographs of ancient monuments.
2. Implement image processing techniques to enhance the visibility of cracks in images.
3. Train and optimize the machine learning model to accurately classify cracked and uncracked images.
4. Evaluate the performance of the proposed approach and compare it to existing manual inspection methods.

By addressing these objectives, we aim to contribute to the advancement of heritage conservation practices and provide a valuable tool for preserving our cultural heritage for future generations

2. Related Work

In India, like in other parts of the world, the historic built environment is mostly composed of bricks, mortar, and stones, among other common construction materials. [28] Much discussion has centred on the decay and degrading propensity of masonry materials and the qualities associated with their evolution. Deterioration of cultural heritage sites is caused by many different things, including the environment, people, weather, and so on. Beams and concretes have had their degradation and cracking processes investigated as part of the proposed study. Beams and concrete constructions deteriorate over time under continuous tension and cyclical loads. Clearly, the fractures have worsened as a consequence of the persistent stress. This makes the timely detection of such problems crucial for the preservation of both the buildings and the landscapes upon which they stand. An exhaustive evaluation of destructive and nondestructive techniques has been planned. Non-destructive and destructive procedures are two ways to assess the degradation of cultural assets, respectively [29]. Destructive methods include transmitted light microscopy, X-ray diffraction, and scanning electron microscopy [30]. A large amount of the monument would have to be destroyed if the aforementioned processes, which involve taking samples from monument structures and transferring them to a scientific institution for study, were really carried out. Such a method would be inappropriate for the monument surveys [31]. The fracture has been identified and classified using both destructive and nondestructive techniques [32]. The Schmidt hammer is a non-destructive tool that can measure the stone's hardness. Ultrasonic imaging, infrared thermography, 3D terrestrial laser scanning, and image processing are further examples of non-destructive technologies [33]. To locate the crack, Brooks et al. (2018) developed a model complete with a thermal imaging camera. The camera was first utilised to distinguish the infrared imprint from the cracks outside, and then it was put to use again to spot the anomalies in the expansive exterior regions [34]. Non-destructive testing (NDT) methods were introduced by Christian Garnier and coworkers in 2011, and those methods were used to composite specimens to pinpoint the defect. The damaged parts were pinpointed in space and time with the help of Graphical Visual Inspection. The depth is determined by using the Ultrasonic Testing Method [35], which is one of three techniques (the others being infrared thermography and ultrasonic tomography) examined in this investigation. Heshan et al. suggested using the Make3D tool set as a unique method for estimating fracture depth (2018). With the aid of the toolkit, it was possible to transform 2D photographs into 3D pictures. The laser scanner was used to get ground truth values, and supervised learning was used to train and classify the model [36].

Dare et al. created a method for automating the process of identifying fractures in concrete structures (2006). Bilinear interpolation was utilised to compute the values of the crack pixels, and the DOG filter was employed to measure the subpixels [37]. In 2017, Hweekwon et al. revealed a method they had devised for detecting cracks in pressed boards. The edge lines have been removed from the sample board and the differences between the two versions are discussed. This approach [38] is a great advance over older techniques since it makes finding and evaluating cracks much faster. Tian Qinggue et al. devised a technique that can detect multiple fractures (2019). In the first stage of the proposed process, edge identification and seed growth are combined. After that, we carried out the skeleton optimization operation, during which time we got rid of anything that wasn't a crack and brought back the crack's properties. Several cracks in the concrete were repaired using this state-of-the-art method. This model classified the discovered bone segments after differentiating the fracture using a mixed input. It was shown to be very useful in evaluating the structural integrity of buildings [39]. A novel approach of measuring the extent, location, and shape of metal defects was developed by Aslam et al. (2020). Median filtering was used to get the desired result of silence. CNN was used to create a segmented image of the damage to the metal so that it could be identified. There was a 93% percentage of correct predictions in the suggested research [40]. Talab et al., (2016) suggested an image processing-based method for identifying concrete fractures in buildings. The major cracks were located using the OTSU method, and the remaining noise was filtered out using a Sobel filter. This area was not suitable for the identification of hairline fractures [41]. Sankarasrinivasan et al. (2015) proposed using HSV thresholding in conjunction with the Bottom Hat Transform to detect cracks in civil buildings. Unmanned aerial vehicles and image processing methods have been merged using combined thresholding to analyse the data and pinpoint the location of fractures. Both small and large surface cracks may be detected using the combination method. However, optimisation of the structural element's size and the threshold value during the process is required [42].

Multiclass support vector machines (SVMs) have been used to classify monument degradation, leading to the introduction of a novel approach based on moments and the degree of colour change for assessing the severity of fractures and moss growth. Degradation detection, classification, identification, and evaluation automation are at the heart of the work described here. The amount of the damage and the monument's value are calculated in order to design the recovery procedure is less matched. In order to improve the impedance matching and creating the operating bands at Ka and Ku bands the split ring resonator is prited along with the stub. The SRR is printed in the maximum surface current area of the stub, which in turn induces the SRR. Thus the proposed antenna with SRR has three operating bands with good impedance matching. The operating frequency of ant b is from 18.91 GHz to 20.30 GHz, 22.84 GHz to 36.41 GHz and 38.18 GHz to 50.80 GHz.

3. Proposed Framework

3.1 Crack detection

The historic built environment in India, and to a lesser extent in other parts of the world, is comprised of a wide variety of construction materials, including bricks, mortar, and stones. [28] There has been much discussion regarding the decay and degrading susceptibility of masonry materials and the characteristics associated with the transformation of such materials. Cultural heritage sites deteriorate for several reasons, including exposure to the elements, vandalism, and neglect. Work has been proposed that investigates the degradation and cracking of structures like beams and concretes. Beams and concrete constructions deteriorate over time under constant tension and cyclical pressure. It is clear that the fractures have widened because of the persistent stress. As a result, it is crucial to detect such problems quickly so that the buildings and landscaping may be preserved for future generations. It has been settled to compare destructive and nondestructive techniques extensively. Surveying the degradation of cultural monuments may be done in two ways: non-destructively and destructively [29]. Methods like as transmitted light microscopy, X-ray diffraction, and scanning electron microscopy are all examples of destructive techniques [30]. Removal of samples from monument structures and their transportation to a research centre for study is part of the aforementioned processes; nevertheless, this operation, if followed out, would lead to the loss of a substantial piece of the monument's construction. Such a method is not what is needed to properly assess the monuments [31]. In order to locate and categorise the fracture, several destructive and nondestructive techniques have been used [32].

The hardness of the stone may be measured using a non-destructive method like the Schmidt hammer. Ultrasonic imaging, infrared thermography, three-dimensional terrestrial laser scanning, and digital image processing are all examples of non-destructive technology [33]. Brooks et al. (2018) constructed a model using a thermal camera to locate the crack. The camera was utilised to tell the infrared imprint of the crack's outside apart from the inside, and then the same camera was used to pick out the anomalies in the larger exterior spaces [34]. Nondestructive testing (NDT) techniques were described by Christian Garnier and colleagues (2011), and these methods were used to detect the defect in composite specimens. Graphical Visual Inspection was utilised to pin down the precise

area and spot where the broken parts were hiding. In this investigation, we employ the Ultrasonic Testing Method [35] to assess depth based on an analysis of findings from three separate techniques: infrared thermography, ultrasonic testing, and shearography. For a fresh take on estimating fracture depth, Heshan et al. suggest using the Make3D tool package (2018). With the aid of the toolkit, 2D photographs have been converted into 3D ones. In this method, supervised learning was used to train and classify the model using ground truth values obtained from the laser scanner [36].

In order to speed up the process of identifying cracks in concrete structures, Dare et al. devised an automated method (2006). The DOG filter was utilised to measure the sub-pixels, and the bilinear interpolation method was employed to analyse the crack pixel values [37]. The method for detecting cracks in pressed boards was reported by Hweekwon et al. (2017). The original form of the sample board is contrasted to one in which the edge lines have been removed. This approach [38] is a vast advance over prior methods, allowing for the faster detection and evaluation of cracks. The technique developed by Tian Qinggue et al., which can detect multiple fractures (2019). The proposed method started with a stage that combined the edge detection and seed growing processes. Once it was complete, the skeleton optimization process was run, during which time the non-crack sections were removed and the crack characteristics were reclaimed. Using this cutting-edge method, we were able to repair many cracks in the concrete. Using a mixed-input method, our model distinguished between fracture types and classified the identified skeletal-based segments accordingly. It worked quite well for evaluating the strength of the buildings [39]. Aslam et al. (2020) developed a novel approach to quantifying the shape, size, and location of metal defects. Median filtering was used to get rid of the noises. CNN was used to divide apart the metal damage and identify specific areas of corrosion. The suggested study had a 93% success rate in terms of accuracy [40]. Talab et al., (2016) suggested a method that makes use of image processing to identify concrete fractures. Important cracks were located using the OTSU method, and the resulting data was then sent through a Sobel filter to eliminate any unwanted background noise. There was no way to see whether there were any hairline fractures here [41]. Sankarasrinivasan et al. (2015) solved the problem of identifying a fracture in civil projects by advocating the use of HSV thresholding in conjunction with the Bottom Hat Transform. Crack detection using integrated unmanned aerial vehicles and image processing methods, including coupled thresholding analysis. The combined method is effective in locating surface cracks of all sizes. However, during the process [42], it is essential to optimise both the size of the structural element and the threshold value.

Multiclass support vector machines (SVMs) have been utilised to classify monument degradation; as a consequence, a novel approach is proposed for assessing crack and moss damage based on moments and the degree to which colours have changed. The purpose of this research is to recognise, classify, and evaluate deterioration in an automated fashion. The amount of the damage is evaluated, and the monument's value is calculated, so that the process of restoring the structure may begin. The historic built environment in India, and to a lesser extent in other parts of the world, is comprised of a wide variety of construction materials, including bricks, mortar, and stones. [28] There has been much discussion regarding the decay and degrading susceptibility of masonry materials and the characteristics associated with the transformation of such materials. Cultural heritage sites deteriorate for several reasons, including exposure to the elements, vandalism, and neglect. Work has been proposed that investigates the degradation and cracking of structures like beams and concretes. Beams and concrete constructions deteriorate over time under constant tension and cyclical pressure. It is clear that the fractures have widened because of the persistent stress. As a result, it is crucial to detect such problems quickly so that the buildings and landscaping may be preserved for future generations. It has been settled to compare destructive and nondestructive techniques extensively. Surveying the degradation of cultural monuments may be done in two ways: non-destructively and destructively [29].

Methods like as transmitted light microscopy, X-ray diffraction, and scanning electron microscopy are all examples of destructive techniques [30]. Removal of samples from monument structures and their transportation to a research centre for study is part of the aforementioned processes; nevertheless, this operation, if followed out, would lead to the loss of a substantial piece of the monument's construction. Such a method is not what is needed to properly assess the monuments [31]. In order to locate and categorise the fracture, several destructive and nondestructive techniques have been used [32]. The hardness of the stone may be measured using a non-destructive method like the Schmidt hammer. Ultrasonic imaging, infrared thermography, three-dimensional terrestrial laser scanning, and digital image processing are all examples of non-destructive technology [33]. Brooks et al. (2018) constructed a model using a thermal camera to locate the crack. The camera was utilised to tell the infrared imprint of the crack's outside apart from the inside, and then the same camera was used to pick out the anomalies in the larger exterior spaces [34]. Nondestructive testing (NDT) techniques were described by Christian Garnier and colleagues (2011), and these methods were used to detect the defect in composite specimens. Graphical Visual Inspection was utilised to pin down the precise area and spot where the broken parts were hiding. In this investigation, we employ the Ultrasonic Testing Method [35] to assess depth based on an analysis of findings from three separate techniques: infrared thermography, ultrasonic testing, and shearography. For a fresh take on

estimating fracture depth, Heshan et al. suggest using the Make3D tool package (2018). With the aid of the toolkit, 2D photographs have been converted into 3D ones. In this method, supervised learning was used to train and classify the model using ground truth values obtained from the laser scanner [36].

In order to speed up the process of identifying cracks in concrete structures, Dare et al. devised an automated method (2006). The DOG filter was utilised to measure the sub-pixels, and the bilinear interpolation method was employed to analyse the crack pixel values [37]. The method for detecting cracks in pressed boards was reported by Hweekwon et al. (2017). The original form of the sample board is contrasted to one in which the edge lines have been removed. This approach [38] is a vast advance over prior methods, allowing for the faster detection and evaluation of cracks. The technique developed by Tian Qinggue et al., which can detect multiple fractures (2019). The proposed method started with a stage that combined the edge detection and seed growing processes. Once it was complete, the skeleton optimization process was run, during which time the non-crack sections were removed and the crack characteristics were reclaimed. Using this cutting-edge method, we were able to repair many cracks in the concrete. Using a mixed-input method, our model distinguished between fracture types and classified the identified skeletal-based segments accordingly. It worked quite well for evaluating the strength of the buildings [39]. Aslam et al. (2020) developed a novel approach to quantifying the shape, size, and location of metal defects. Median filtering was used to get rid of the noises. CNN was used to divide apart the metal damage and identify specific areas of corrosion. The suggested study had a 93% success rate in terms of accuracy [40]. Talab et al., (2016) suggested a method that makes use of image processing to identify concrete fractures. Important cracks were located using the OTSU method, and the resulting data was then sent through a Sobel filter to eliminate any unwanted background noise. There was no way to see whether there were any hairline fractures here [41]. Sankarasrinivasan et al. (2015) solved the problem of identifying a fracture in civil projects by advocating the use of HSV thresholding in conjunction with the Bottom Hat Transform. Crack detection using integrated unmanned aerial vehicles and image processing methods, including coupled thresholding analysis. The combined method is effective in locating surface cracks of all sizes. However, during the process [42], it is essential to optimise both the size of the structural element and the threshold value.

Multiclass support vector machines (SVMs) have been utilised to classify monument degradation; as a consequence, a novel approach is proposed for assessing crack and moss damage based on moments and the degree to which colours have changed. The purpose of this research is to recognise, classify, and evaluate deterioration in an automated fashion. The amount of the damage is evaluated, and the monument's value is calculated, so that the process of restoring the structure may begin.

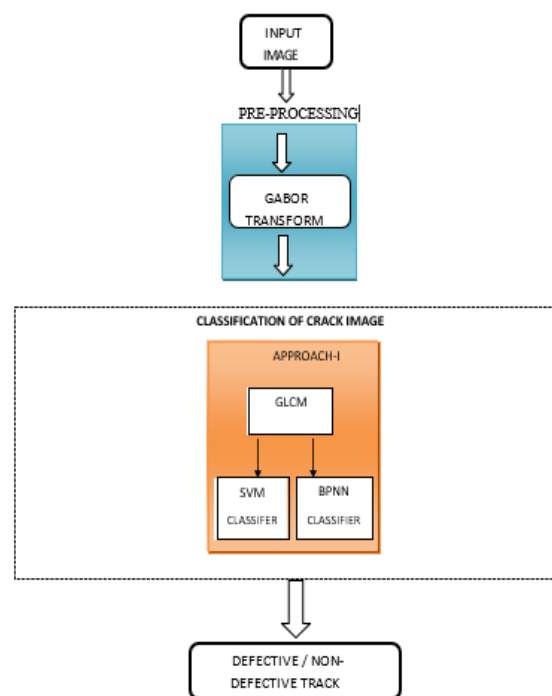


Figure. 2 Proposed Crack Detection System

1.2 Pre-processing

It enhances the image, allowing the hole to be more easily seen. The captured image is then converted to monochrome form. An Adaptive Histogram Equalization (AHE) technique was used to smooth out the damage in the image. This is achieved by boosting the image's contrast, which converts the image's colour value to an intensity value

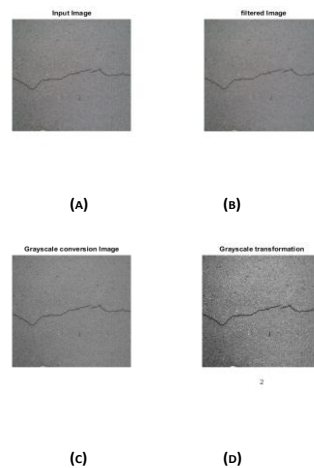


Figure. 3. (a) Image with Crack (b) Pre-processed Image of (a), (c) grey scale transformation, (d) Pre-processed Image of grey scale.

3.3 Gabor Transform

The spatial domain image is converted into an amplitude, frequency, and phase multi resolution image using the multi resolution transform. After that, you may use the picture with several resolutions. Traditional multi resolution transforms including the discrete wavelet transform (DWT), contourlet, and curvelet were used to convert the spatial domain picture into a multi resolution image, but the results were less than ideal. The spatial domain image of the Ancient Structure is transformed using the Gabor transform so that the multi resolution picture may be extracted. This is done to avoid the limitations of common classifiers.

Four different scales (= 1, 2, 3, 4) and four different orientations (= 45 degrees, 90 degrees, 120 degrees, 180 degrees) are used to construct the Gabor kernels used in this investigation. In mathematics, $g(x,y)$ stands for the Gabor kernel, which is defined as,

x and y are the pixel coordinates, and σ is the standard deviation.

$$\begin{bmatrix} Y \\ C_b \\ C_r \end{bmatrix} = \begin{bmatrix} 0 \\ 128 \\ 128 \end{bmatrix} + \begin{bmatrix} 0.299 & 0.587 & 0.114 \\ -0.169 & -0.331 & 0.500 \\ 0.500 & -0.419 & -0.081 \end{bmatrix} \cdot \begin{bmatrix} R \\ G \\ B \end{bmatrix} \quad (1)$$

where Y is the luminance of the RGB image; C_b is the chrominance of the B component; C_r is the chrominance of the R component, respectively. In post processing stage (at the end of background subtraction algorithm), each luminance image is converted back to RGB image using the following equation as,

$$\begin{bmatrix} R \\ G \\ B \end{bmatrix} = \begin{bmatrix} 1.000 & 0.000 & 1.400 \\ 1.000 & -0.343 & -0.711 \\ 1.000 & 1.765 & 0.000 \end{bmatrix} \cdot \begin{bmatrix} Y \\ C_b - 128 \\ C_r - 128 \end{bmatrix} \quad (2)$$

The Gabor magnitude image and its phase or orientation image at 45° are shown in Fig. 4 (a), (c) and Fig. 4 (b), (d) respectively

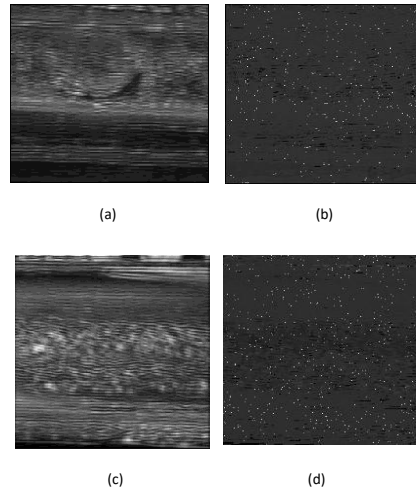


Figure. 4. (a) and (c) Gabor Magnitude Image with Crack and Without Crack (b) and (d) Gabor Orientation Image with Crack and Without Crack

Complex

$$g(x, y; \lambda, \theta, \psi, \sigma, \gamma) = \exp\left(-\frac{x'^2 + \gamma^2 y'^2}{2\sigma^2}\right) \exp\left(i\left(2\pi \frac{x'}{\lambda} + \psi\right)\right) \quad (3)$$

Real

$$g(x, y; \lambda, \theta, \psi, \sigma, \gamma) = \exp\left(-\frac{x'^2 + \gamma^2 y'^2}{2\sigma^2}\right) \cos\left(2\pi \frac{x'}{\lambda} + \psi\right) \quad (4)$$

Imaginary

$$g(x, y; \lambda, \theta, \psi, \sigma, \gamma) = \exp\left(-\frac{x'^2 + \gamma^2 y'^2}{2\sigma^2}\right) \sin\left(2\pi \frac{x'}{\lambda} + \psi\right) \quad (5)$$

where

$$x' = x \cos \theta + y \sin \theta \quad (6)$$

and

$$587 \times 44' = -x \sin \theta + y \cos \theta \quad (7)$$

3.3 Ancient Monument Image Feature Extraction

Features are derived from the Gabor magnitude image and used to distinguish the cracked picture from the non-cracked picture based on its energy characteristics. These characteristics are used to evaluate the dissimilarities between the pictures. Local Binary Patterns (LBP) and Grey Level Co-occurrence Matrix (GLCM) features are extracted from the Gabor magnitude image and used for crack picture classifications in this study.

3.3.1 Grey Level Co-occurrence Matrix (GLCM)

Most of the previous methods for extracting texture characteristics are linked to tunable parameters, and a plethora of options are now available for doing so. It might be difficult to ascertain which feature extraction methods are best suited to a certain task and which parameters should be used to get optimal results. Finding the optimal combination of "feature extraction and classification" is difficult since the effectiveness of classification approaches is also reliant on the difficulties. Experimentation is commonly used to evaluate which of many feature extraction approaches is most effective in a specific scenario. The proposed inspection method employs the texture feature to build robust and discriminating feature descriptors of the Ancient Monument's exterior. These features are extracted using techniques like Local Binary Pattern (LBP) and Gray Level Co-occurrence Matrix (GLCM).

The GLCM matrix, like the different angles, may be differentiated in a variety of ways. Each pixel is comprised of eight neighbours, giving you a total of eight possible angles: 0, 45, 90, 135, 180, 225, 270, and 315 degrees.

The matrix coefficients on either the top or bottom diagonal may be used to create the vectors, which is convenient since the matrices are symmetric. As a result, if we set equal to 0 degrees, we would get the same number of occurrences of pairs as if we set equal to 180 degrees. 45-degree, 90-degree, and 135-degree angles are all included in this concept. This means that there are four possible values for that may be chosen. When the image being analysed is isotropic or when directional information is unnecessary, an isotropic GLCM may be created by integrating across all possible angles. After trying many orientations, it was discovered that testing for Ancient Monument faults at 45 degrees best recreated the fracture appearance. As a result, only characteristics in the 45-degree orientation are retrieved individually to speed up the computing process.

Using the Gabor magnitude picture at different orientations of pixels inside the image, a GLCM matrix may be constructed, from which the GLCM features can be extracted. Included in these are the zero, forty-five, ninety, and thirteen-five degree orientations. The GLCM matrix used in this study has pixel orientations of 450 degrees. The greatest pixel value in the Gabor magnitude image is used to establish the number of rows and columns in the GLCM matrix. Then, 450 orientations are performed for each pixel value in the Gabor orientation image to generate the values for the GLCM table.

After the GLCM matrix is calculated, characteristics such as contrast, energy, entropy, and correlation may be extracted. Pixel-to-pixel intensity differences throughout an entire image are quantified using contrast (CT). All of the image's pixels are considered. The contrast value is zero in a static image. The opposite of entropy is energy (E), which quantifies local homogeneity. The letter E represents the concept of energy. This quality will sum up how consistent the texture is. EP, or entropy, is a statistical measure of a system's disorder (how regular the pixel values are within the window). The texture of a picture may be described in a variety of ways using this statistical measure of unpredictability. Despite its common classification as a first-degree measure, it more accurately belongs in the category of zero-degree measures. A pixel's level of association with its neighbouring pixels throughout the whole image is quantified by a statistic called correlation (C). This is the correlation equation. Values of the correlation coefficient might be anything from -1 to 1.

Table 1 displays the GLCM features recovered from the Gabor magnitude Ancient Monument picture as well as the technique used to extract those features. Algorithm 1's sample photos include both undamaged and damaged versions of the Ancient Monuments utilised in the demonstration.

Algorithm 1: GLCM Algorithm

<p>Input:</p> <p>Gabor Transformed Image (Img1).</p> <p>Process:</p> <p>Step 1: Get input rail track image with grey level L.</p> <p>Step 2: Construct the $L \times L$ GLCM matrix p_d.</p> <p>Step 3: The values of GLCM matrix $P_d(i, j)$, ($i, j=0,1,2,\dots,L-1$) is defined as the frequency of that two pixels i and j respectively at the orientation θ of 45degree.</p> <p>Step 4: Extract Contrast, Correlation, Energy and Homogeneity feature values from the GLCM matrix</p> <p>Step 5: Apply step1 to step 4 for both normal and abnormal rail track images.</p> <p>Output:</p> <p>Features set (Contrast F1, Correlation F2, Energy F3, and Homogeneity F4).</p> <p>Step 6 Find normalized GLCM matrix at the orientation of 45 degree</p>

Table 1: GLCM features for Normal and Cracked Ancient Monument Test Image Sample

GLCM Features	Cracked	Non-Cracked
Contrast	8.17×10^3	2.19×10^4
Correlation	-0.0072	0.02
Energy	3.21×10^{-5}	2.38×10^{-5}
Homogeneity	0.092	0.012

3.1.1 Local Binary Patterns(LBP)

Using LBP as a feature extraction method has several advantages. To begin, the LBP technique is very adaptable and resistant to monotonic changes in grey-level, lighting, scaling, perspective, and rotation. Second, because of its computational simplicity, the LBP approach makes real-time picture analysis possible in demanding environments. In reality, the LPB's excellent discriminating capacity comes at a lower computing cost than that of its SIFT and SURF analogues. Last but not least, the LBP has shown to be very effective in a wide range of applications, including facial identification, emotion analysis, texture classification, and motion analysis.

The central pixel is linked to its neighbours by this function. The binary patterns are generated by comparing all of the neighbouring pixels to the central one. If the surrounding pixels are of a larger magnitude than the central pixel, a binary 1 will be generated, and if they are of a lesser magnitude, a binary 0 will be generated. The binary pattern of these eight bits represents a single decimal number. Table 1 explains the LBP feature extraction technique, and Fig. 5 depicts the LBP feature extraction using algorithm 2 for a piece of a picture of an ancient monument.

$$F_{LBP} = \sum_{p=0}^{P-1} f(I_p - I_c)2^p$$

$$f(x) = \begin{cases} 1; & x \geq 0 \\ 0; & x < 0 \end{cases} \quad (8)$$

where, I_p and I_c are the intensity value of the neighbourhood pixel and centre pixel respectively and P is the number of samples on the circle of radius ' r '.

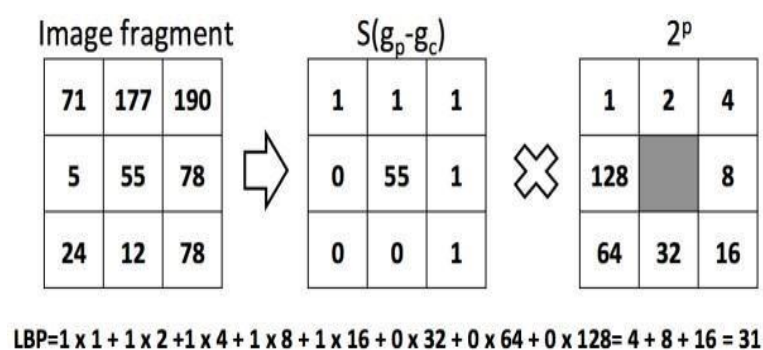


Figure. 5. Sample Test Image LBP Calculation

The steps necessary to get the LBP characteristic are detailed in Algorithm 2. To train a classifier, we feed it a picture of the Ancient Monument that has had its Gabor features removed.

Algorithm 2: LBP Algorithm**Input:**

Gabor Transformed Image (Img1).

Step 1: Get Gabor transformed rail track image in multi resolution format.

Step 2: Split the entire Gabor transformed image into number of sub modules whose window size is 3×3.

Step3: In the resulting 3×3 sub image the value of the center pixel g_c is compared with the neighboring pixels g_p .

Step 4: If the neighboring pixel g_p has a value greater than the center pixel g_c , then the neighboring pixel value is replaced by 1.

$$s(g_p - g_c) = 1; \text{ if } g_p \leq g_c$$

Step 5: If the neighboring pixel g_p has a value less than the center pixel g_c , then the neighboring pixel value are replaced by 0.

$$s(g_p - g_c) = 0; \text{ if } g_p > g_c$$

Step 6: In this way all the neighboring pixels will be replaced by either 0 or 1, combining which we get an eight digit binary number using the Equation.

Step 7: This eight digit binary number is converted into decimal and the decimal value is used to replace the centrepixel.

Step 8: Move the sub window to next adjacent pixel until last pixel in the image.

Output:

LBP feature extracted image

When evaluating the consistency of an LBP pattern, the number of times it must be bitwise converted from 0 to 1 or 1 to 0 is used. If the uniformity measure of a local binary pattern is exactly 2, we refer to it as uniform. In contrast to the non-uniformity of patterns like 11010001 (4 transitions) and 01010111 (6 transitions), patterns like 00000000 (0 transitions), 11111111 (0 transitions), 01110000 (2 transitions), and 11000111 (2 transitions) are uniform. Uniform LBP mapping involves assigning a unique output label to each uniform pattern while assigning a single label to all non-uniform patterns. Therefore, for patterns of P bits, the total number of possible mapping

output labels is $P(P-1) + 3$. The uniform mapping yields 59 (Fig. 5) output labels for areas with 8 sample points and 243 labels for areas with 16 sampling points. One possible statement of the principle is as follows: Equation

$$(9): \text{LBPriu2} = \begin{cases} P_r p^{-1} S(g_p - g_c), & U \leq 2 \\ P + 1, & \text{otherwise} \end{cases} \quad (9)$$

The benefit of LBP^u detects only the important local textures, like spots, line ends, edges and corners

3.4 Modelling of Ancient Monument Image Classification

A classifier is employed to determine whether or not the active image of the Ancient Monument is fractured. In this research, a photograph of an antique monument is classified using two different classifiers: a Support Vector Machine (SVM) and a Back Propagation Neural Network (BPNN). The image of the Ancient Monument was classified using convex classifiers like Principal Component Analysis (PCA) so that defects could be identified, however the classification accuracy was low.

3.4.1 Back Propagation Neural (BPNN)

It has ties to machine learning and AI and excels in solving issues that might otherwise be intractable with more conventional methods. Artificial neural networks might be used to find answers to these sorts of difficulties. Simple nerve cells that are coupled to one another make up the memory and recognition centre of the brain. In [55], an efficient model termed Back Propagation Neural Networks was (BPNN). There are three parts to a typical BPNN: the input layer, the hidden layer, and the output layer. How smart a neural network really is depends on the values of the weights used to connect its neurons. The BPNN can learn from examples and adjust the weights of its neurons in response to error back propagation, allowing it to essentially educate itself. Using (FFBP) neural network, this research finds instances of damage to old structures in pictures. Both training and testing modes are available for use with these neural s. This classifier is trained by combining the characteristics collected from cracked and uncracked images of Ancient Monuments. During the testing phase, the classifier classifies the extracted features from the active Ancient Monument image based on the learnt pattern, outputting a low (0) or high (1) result. A low value for this classifier (0, for example) indicates that the test image does not include any cracks, whereas a high value (1, for example) indicates that the image does contain cracks.

Improved Support Vector Machine (ISVM)

Support vector machines (SVMs) are a kind of supervised machine learning that have many potential uses, including but not limited to regression, classification, and outlier detection. In this research project, a support vector machine (SVM) was used to identify whether or not a photograph of a historical landmark showed any signs of cracking. SVM that relies on finding the hyperplane that best divides the dataset into two groups, such as pictures of ancient monuments that have cracks and pictures of the same structures without cracks. By dividing the information into training points with the largest distance from the hyperplane and the training points closest to the hyperplane, the support vector machine (SVM) technique trains linear machines to identify an ideal hyperplane. Training points closest to the optimal separation hyperplane are referred to as support vectors. Figure 2 depicts the SVM architecture.

Here, we begin with the linear example and then go on to the nonlinear situation. Here is a definition of the necessary training dataset:

$$D = (X_i, y_i) \mid X_i \in R^p, y_i \in \{-1, 1\}, \quad (10)$$

Where, X , is a real n -dimensional vector and y_i takes either 1 or -1 . Now, W be a normal vector (or weight vector) to the hyperplane and b be a bias then with the help of dot product, equation of the hyperplane can be written as below:

$$W \cdot X + b = 0 \quad (11)$$

Equations of PSP and NSP respectively are given below:

$$W \cdot X + b = 1 \quad (12)$$

$$W \cdot X + b = -1 \quad (13)$$

Distance between PSP and NSP is $\frac{2}{|W|}$, therefore to maximize the margin we have to minimize $|W|$.

Thus, to strictly signify the training data points that lie within the sides of PSP and NSP are given by the following inequalities:

$$W \cdot X_c + b \geq 1 \quad \text{where} \quad y_2 = 1 \quad (14)$$

W. $X_d + b \leq -1$ where $y_c = -1$ (15)
 Combining inequalities 14,15 we get

$$y_i(W \cdot X_v + b) \geq 1, \forall 1 \leq i \leq n \quad (16)$$

Now, finally the optimization problem can be stated as below: Subject to the constraint

$$y_2(W, X_4 + b) \geq 1, \forall 1 \leq n \quad (17)$$

$$\arg \min_{n \rightarrow \infty} \max \left\{ \frac{1}{2} \| \cdot \|^2 - \sum_{i=1}^1 \alpha_i [y_i(W, X_i + b) - 1] \right\} \quad (18)$$

Where α_i is Lagrange Multipliers and W can be defined as below:

$$W = \sum a_2 y_2 X_1 \quad (19)$$

Input patterns are transformed into a higher-dimensional feature space via SVM's use of nonlinear mapping. In the testing phase of this classifier, the extracted features from the live image of the Ancient Monument are sorted according to the learnt pattern, and the classifier returns a 0 or 1 based on the category. If the value of this classifier is low, 0, it is likely that the test photo does not include any cracks, whereas if it is high, 1, cracks are present in the picture.

The selection of GLCM and LBP features for classification was based on their proven effectiveness in capturing textural information relevant to crack detection in images of ancient monuments. GLCM features, including contrast, correlation, energy, and homogeneity, provide valuable insights into the spatial distribution of pixel intensities and the texture of image regions. These features are particularly well-suited for capturing the intricate patterns and variations associated with cracks in stone structures.

Similarly, LBP features encode information about local patterns and textures by quantifying the distribution of intensity variations within image neighborhoods. By considering the binary patterns formed by comparing pixel intensities with their neighbors, LBP features can effectively capture the distinctive textural properties of cracks, such as their roughness and continuity.

The selection of specific GLCM and LBP features for classification was guided by their ability to discriminate between cracked and uncracked regions in ancient monument images. Features that exhibited strong discriminative power, as measured by statistical metrics or domain knowledge, were prioritized for inclusion in the classification model.

Moreover, the choice of features may have been influenced by considerations such as computational efficiency, robustness to noise and image variations, and interpretability of results. Features that could be efficiently computed and provided meaningful insights into the underlying texture characteristics of cracks were preferred for inclusion in the classification process.

Overall, the feature selection process aimed to identify a set of discriminative GLCM and LBP features that could effectively differentiate between cracked and uncracked regions in images of ancient monuments. By leveraging these features, the classification model could accurately identify and classify cracks, contributing to the overall effectiveness of the proposed approach for automated crack detection and classification.

3.5 Proposed approaches for Ancient Monument Image Classification

Classification of Ancient Monument Image Algorithm I (AMCD I), Classification of Ancient Monument Image Algorithm II (AMCD II), and Classification of Ancient Monument Image Algorithm III are the methods that have been presented for detecting cracks in Ancient Monuments (AMCD III). AMCD I was implemented using the GLCM feature, AMCD II was implemented using the LBP feature, and AMCD III was created using a fusion of the GLCM and LBP features.

The training and evaluation of the classifiers likely involved a combination of techniques, including cross-validation or hold-out validation. Here's a typical approach:

1. Training the Classifiers: Initially, the classifiers, such as Support Vector Machines (SVMs) and Neural Networks (NNs), were trained using a portion of the available dataset. This dataset would consist of annotated images, where

each image is labeled as either cracked or uncracked. The classifiers are trained to learn the underlying patterns and relationships between the extracted features (e.g., GLCM and LBP features) and the corresponding class labels.

2. Cross-Validation: Cross-validation is a commonly used technique to assess the performance of machine learning models. In this approach, the dataset is divided into multiple subsets (folds), and the classifiers are trained and evaluated multiple times, each time using a different subset for evaluation and the remaining subsets for training. This process allows for a more robust estimation of the model's performance and helps mitigate overfitting.

3. Hold-out Validation: Alternatively, hold-out validation involves splitting the dataset into two disjoint sets: a training set and a validation set (or test set). The classifiers are trained using the training set and evaluated using the validation set. This approach provides a single estimate of the model's performance on unseen data.

In practice, researchers often employ a combination of cross-validation and hold-out validation to assess the performance of classifiers thoroughly. Cross-validation is typically used for model selection and tuning hyperparameters, while hold-out validation provides a final estimate of the model's performance on unseen data.

The specific details of how the classifiers were trained and evaluated, including the choice of validation technique and any hyperparameter tuning procedures, should be described in the methodology section of the paper to ensure transparency and reproducibility of the results.

3.5.1 Classification of Ancient Monument Image Algorithm-I

Classification of Ancient Monument Image Algorithm-I (AMCD-I) is the first technique that was developed. It combines pre-processing, the Gabor transform, and the GLCM algorithm to build the feature vector as the output. This feature is input into the BPNN and SVM models, which are then used to classify ancient monuments. Algorithm 3 presents the AMCD-I technique that has been suggested.

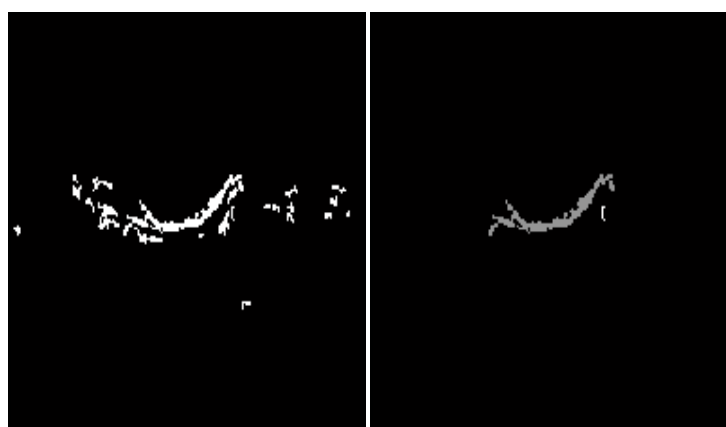
3.1.1 Classification of Ancient Monument Image Algorithm-II

The second method under consideration preprocessing, the Gabor transform, and the LBP algorithm are included in the Classification of Ancient Monument Image Algorithm-II (AMCD-II) in order to construct the feature vector as the output of the algorithm. This characteristic is included into BPNN and SVM models for the purpose of ancient monument classification.

Classification of Ancient Monument Image Algorithm-

Third proposed approach Classification of Ancient Monument Image Algorithm-III (AMCD-III) includes pre-processing, Gabor transform, and Feature extraction using GLCM and LBP algorithm. This Combined feature is applied to BPNN and SVM model for classification of Ancient Monument .

Further, the cracks in the classifier image are detected using morphological operations. It produces dilation and erosion images, which subtracts the eroded image (Fig.6(b)) from the dilated image (Fig. 6(a)) to obtain the cracked regions in the classified image (Fig. 6(c)). The bounding box drawn over the cracked region for better identification.



(a)

(b)



(c)

Figure 6. (a) Morphologically Processed Dilated Image (b) Eroded Image(c) Crack Segmented Image

4. Results and Discussion

There are a few well-known public datasets that have been extensively used and researched as a benchmark for comparing various strategies and methods used in other types of maintenance domains. These datasets may be found online. On the other hand, there are only a few tiny datasets accessible for Ancient Monument flaws, and the datasets that researchers often utilise are typically confidential and cannot be shared. The dataset that was used in this suggested study is comprised of three hundred pictures of an Ancient Monument that were produced in real time. Images were taken using a Canon EOS 1500D 24.1 digital single-lens reflex camera at top angles of 450, 900, and 1350 degrees with regard to the surface of the Ancient Monument. In addition, the collection is divided into two groups: one contains 150 photographs of ancient monuments with cracks, while the other has 150 images of ancient monuments without cracks. Both groups' images have a resolution of 128 by 128 pixels.

When using classification techniques, it is essential to keep the data used for training and testing separate so that the findings are not skewed. The k-fold cross-validation technique (shown in fig.7) is a well-known assessment strategy that uses many independent sets. A total of k evaluations are carried out on the picture once it has been folded into the specified number of folds, with each fold being put to use for testing while the remaining folds (k minus 1) are put to use for training. The example may be seen in the figure labelled. For the purpose of classifier assessment in this study, a 4-fold cross-validation approach is used. The picture dataset is split up into four sections, with each section containing 75 photos. The performance of the proposed crack detection system is evaluated with regard to ground truth pictures in terms of sensitivity, specificity, and accuracy.

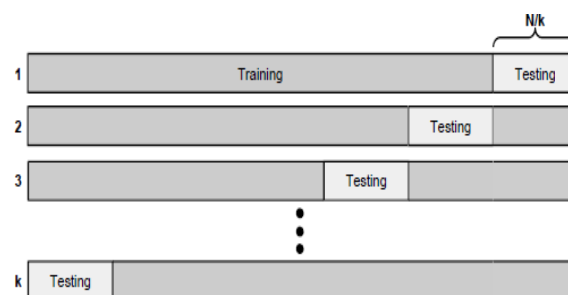


Figure 7. Illustration for k-fold Cross-Validation.

Confusion matrices must be developed before one can determine the sensitivity, specificity, and accuracy of a test. Confusion matrices not only give information on samples that were properly categorised and samples that were mistakenly classified, but they also provide information on which class the inaccurate classification was made to. Figure 8 provides a graphic representation of the confusion matrix idea, in addition to the several sorts of categorization findings unique to this study endeavour, are elaborated upon more below: TP stands for "True Positive," which refers to the number of crack pixels that have been appropriately separated. TN stands for "true negative," which refers to the amount of accurately divided pixels that are not cracks. FP stands for "false positive," which refers to the number of crack pixels that have been incorrectly segmented. FN stands for "false negative," which refers to the number of non-crack pixels in Ancient Monument that were segmented incorrectly.

		Predicted	
		Class 1	Class 2
True	Class 1	True positive	False negative
	Class 2	False positive	True negative

Fig. 8. Principle of Confusion Matrix

$$\text{Sensitivity (Se)} = \text{TP} / (\text{TP} + \text{FN}) \quad (20)$$

$$\text{Specificity (Sp)} = \text{TN} / (\text{TN} + \text{FP}) \quad (21)$$

$$\text{Accuracy (Acc)} = (\text{TP} + \text{TN}) / (\text{TP} + \text{FN} + \text{TN} + \text{FP}) \quad (22)$$

Within the framework of the proposed method AMCD I, the GLCM features were extracted from the picture, and the classifiers SVM and BPNN were used to categorise the Ancient Monument photographs. In the proposed method AMCD II, the LBP features were extracted from the picture of the Ancient Monument, and the classifiers SVM and BPNN were used to classify images of Ancient Monuments. In the last step of the proposed method AMCD III, the fusion of the LBP and GLCM features is provided as input to the classifiers SVM and BPNN. This step is intended to classify ancient monuments. The system that was envisioned was realized utilising a computer with an Intel (R) Core (TM) i3 processor operating at 2.20 gigahertz.

Classification of Ancient Monument Images Algorithm I with SVM and BPNN

The GLCM features are retrieved from the GLCM matrix, which may be created directly from the Gabor magnitude picture at various directions of the pixels inside the image. These directions include 0 degrees, 45 degrees, 90 degrees, and 135 degrees. Within the scope of this research project, the GLCM matrix is built with pixel orientations of 450. The entropy, contrast, energy, and correlation characteristics are the ones that are taken from the data. The retrieved features are sent into the classifiers SVM and BPNN so that they may be trained and classified.

Support Vector Machine (SVM)

In order to categorise the data in a linearly separable manner, a linear support vector machine (SVM) is used. The linear classifier based on the SVM makes an effort to optimise the margin that exists between the different hyper planes. Support vectors are the names given to the patterns that are seen on the maximum margins. GLCM is packed with a total of fourteen different features. Only four of the fourteen characteristics were chosen for this study to be employed in the classification of crack-free and cracked photographs of ancient monuments using the support vector machine (SVM).

Back Propagation Neural (BPNN)

During the training process, you will first create and configure a three-layered neural network, and then you will teach it to learn about the extracted characteristics of pictures from the training set. The backpropagation algorithm is used to carry out the learning process, which includes calculating error and changing weights in order to decrease error. This is done in order to maximise accuracy. Establish a neural network (NN) and set its settings as follows: epochs = 1000, learning rate = 90%, allowed error = 0.01.

The suggested method AMCD I's performance was assessed in terms of Accuracy, Sensitivity, and Specificity, as shown in Table 2, which contains the average result from 4 separate assessments. In comparison to the SVM classifier, the BPNN classifier has a classification accuracy that is 88.00 percentage points greater. Again, the suggested AMCD was assessed by myself using a dataset consisting of 100 photos (72 images with cracks and 28 images without cracks), and the results of this evaluation are given as a classification rate. Table 2 presents the classification rate achieved by AMCD I using SVM and BPNN for pictures containing cracks and those that do not include cracks

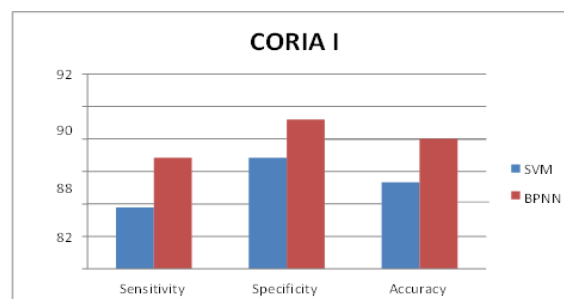
Table 2: Performance of AMCD I

S.No	Model	Sensitivity (in %)	Specificity (in %)	Accuracy (in %)
1	SVM	83.78	86.84	85.33
2	BPNN	86.84	89.19	88.00

Table 3: Classification Rate of AMCD I with SVM and BPNN

Test Image/Approach		AMCDI+SVM	AMCD I+BPNN
with Crack	Actual Tested Images	72	72
	Correctly Detected Images	62	64
	Classification Rate (in %)	86.11	88.89
without Crack	Actual Tested Images	28	28
	Correctly Detected Images	25	25
	Classification Rate (in %)	89.29	89.29
Average Classification Rate (in %)		87.70	89.09

Fig. 9 shows the performance comparison of AMCD I using SVM and BPNN classifier. The Graph shows that AMCD I with BPNN performed better than AMCD I with SVM in terms of Sensitivity and Accuracy.

**Figure 9.** Performance comparison of AMCD I using SVM and BPNN

3.1.4 Classification of Ancient Monument Images Algorithm II with SVM and BPNN

In this method, the LBP features are determined by establishing a correlation between the central pixel and the pixels that surround it. In order to construct the binary patterns, each surrounding pixel is compared with the central pixel. As a consequence of doing the LBP computation across a 3x3 window that spans the whole picture block (128x128), an LBP feature matrix that is 128x128 in size is produced. The size of the feature vector may be increased to 59 when uniform LBP, which is a simplified version of conventional-LBP, is used. The classifiers SVM and BPNN get their information for constructing models from the features that were retrieved from the training dataset pictures. Evaluation of the classifier using the ground truth picture is performed using the testing dataset's features. The performances of the suggested method AMCD II are analysed in terms of accuracy, sensitivity, and specificity, as shown in Table 4. When compared to the SVM, the BPNN classifier results in a classification accuracy that is 92.00% more accurate. Once again, the proposed AMCD II is assessed using a dataset of 100 photos (72 images with cracks and 28 images without cracks), and the results of this evaluation are summarised as a classification rate. Table 4 presents the classification rate achieved by AMCD II using SVM and BPNN for pictures containing cracks and those that do not include cracks.

Table 4: Performance of AMCD II

S.No	Model	Sensitivity (in %)	Specificity (in %)	Accuracy (in %)
1	SVM	89.19	89.47	89.33
2	BPNN	91.89	92.11	92.00

Table 5: Classification Rate of AMCD II with SVM and BPNN

Test Image/Approach		AMCDII+SVM	AMCD II+BPNN
with Crack	Actual Tested Images	72	72
	Correctly Detected Images	65	67
	Classification Rate (in %)	90.28	93.06
without Crack	Actual Tested Images	28	28
	Correctly Detected Images	25	26
	Classification Rate (in %)	89.29	92.86
Average Classification Rate (in %)		89.78	92.96

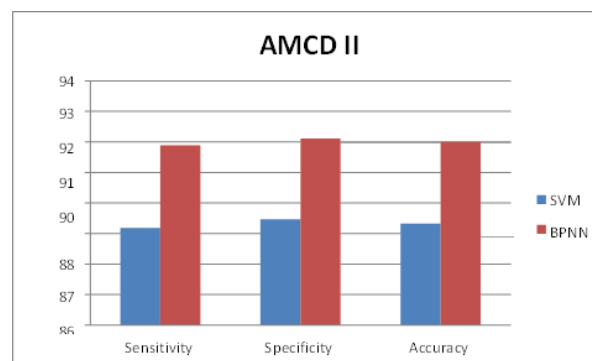
**Figure. 10** Performance comparison of AMCD II using SVM and BPNN

Fig. 10 shows the Performance Graphical comparison of AMCD II using SVM and BPNN classifier. The Graph shows that AMCD II with BPNN performed better than AMCD II with SVM in terms of Sensitivity, Specificity and Accuracy.

Classification of Ancient Monument Images Algorithm III with SVM and BPNN

This research work investigated further the performances of combining GLCM and LBP features because GLCM features are widely used to analyse texture features statistically, and LBP features are perceived to be an easy preservation to generate features. As a result, this research work investigated how well combining GLCM and LBP features works. The classifiers SVM and BPNN are fed the combined features that were generated by GLCM and LBP. The performance of the suggested method, AMCD III, is assessed in terms of accuracy, sensitivity, and specificity, as shown in Table 6.

When compared to the SVM, the BPNN classifier results in a classification accuracy that is 97.33% more accurate. Once again, the proposed AMCD II is assessed using a dataset of 100 photos (72 images with cracks and 28 images without cracks), and the results of this evaluation are summarised as a classification rate. Table 7 presents the classification rate achieved by AMCD III using SVM and BPNN for pictures containing cracks and those that do not include cracks. Table 6 Performance of AMCD III

Table 6 PERFORMANCE OF AMCD III

S.No	Model	Sensitivity (in %)	Specificity (in %)	Accuracy (in %)
1	SVM	92.11	94.59	93.33
2	BPNN	97.37	97.30	97.33

Table 7 Classification Rate of AMCD III with SVM and BPNN

Test Image/Approach		AMCDIII+SVM	AMCD III+BPNN
image with Crack	Actual Tested Images	72	72
	Correctly Detected Images	68	71
	Classification Rate (in %)	94.44	98.61
image without Crack	Actual Tested Images	28	28
	Correctly Detected Images	26	27
	Classification Rate (in %)	92.86	96.43
Average Classification Rate (in %)		93.65	97.52

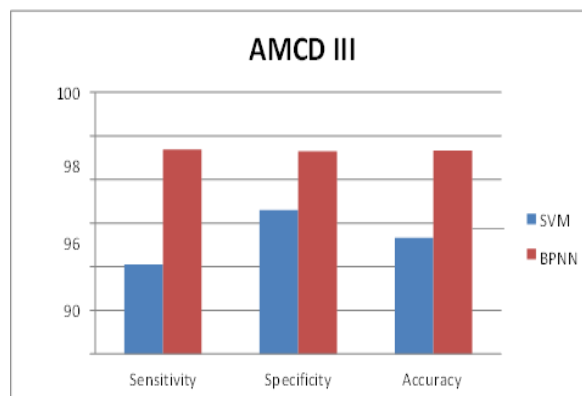


Fig. 11 Performance comparison of AMCD III using SVM and BPNN

Figure 11 presents a graphical comparison of the performance of AMCD III when utilising SVM and BPNN as the classifier. According to the graph, the AMCD III model trained with BPNN performed much better than the AMCD III model trained with SVM in terms of sensitivity, specificity, and accuracy.

The above description makes it abundantly evident that the combination of GLCM and LBP characteristics, which is referred to as AMCD III, results in excellent classification accuracy when used in conjunction with BPNN. The example categorization of a test picture using the suggested method AMCD III in conjunction with BPNN is shown in Figure 12.

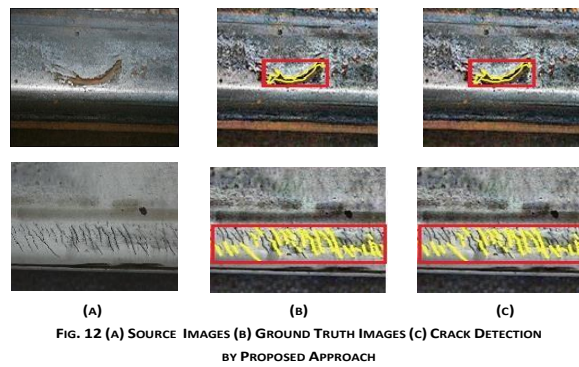


Fig. 12 (a) Source Images (b) Ground Truth Images (c) Crack Detection by Proposed Approach

The proposed approach AMCD I, II, III are all compared with the existing methods as given in Table 8. The performance of the Ancient Monument image classification using AMCD I, II, and III using SVM and BPNN are measured for various Ancient Monument test images. By comparing features and classifiers in Table 8, shows that proposed AMCD III with BPNN yields the better accuracy when compared to other methods.

Table 8. Comparison of the Proposed Approach with State-of-the-art systems

Authors	Number of classes	Surface Type	Feature and Classifier	Accuracy (%)
[46]	7	Reflected Metal	DWT, Fourier Spectral, SVM	85.00
[47]	2	Textile	GLCM, FFNN	91.00
[48]	3	wood	LBP, BPNN	93.30
[49]	2	Ceramic Tiles	UDWT, GLCM	93.20
Proposed approach AMCD I	2	Ancient Monument	GLCM, BPNN	88.00
Proposed approach AMCD II	2	Ancient Monument	LBP, BPNN	92.00
Proposed approach AMCD III	2	Ancient Monument	GLCM, LBP, BPNN	97.33

The suggested system was compared to state-of-the-art approaches for surface crack detection based on four criteria: number of classes, surface types, feature extraction and classifier, and accuracy. Table 8 shows that the proposed method outperformed the alternatives in terms of accuracy. The proposed inspection technique combines LBP and GLCM features to provide robust and discriminative feature descriptors of Ancient Monument surfaces. The BPNN classifier was used to build the classification model. Photos of historic sites were used to test the proposed technology, and the promising findings have given us reason to be optimistic about its future use.

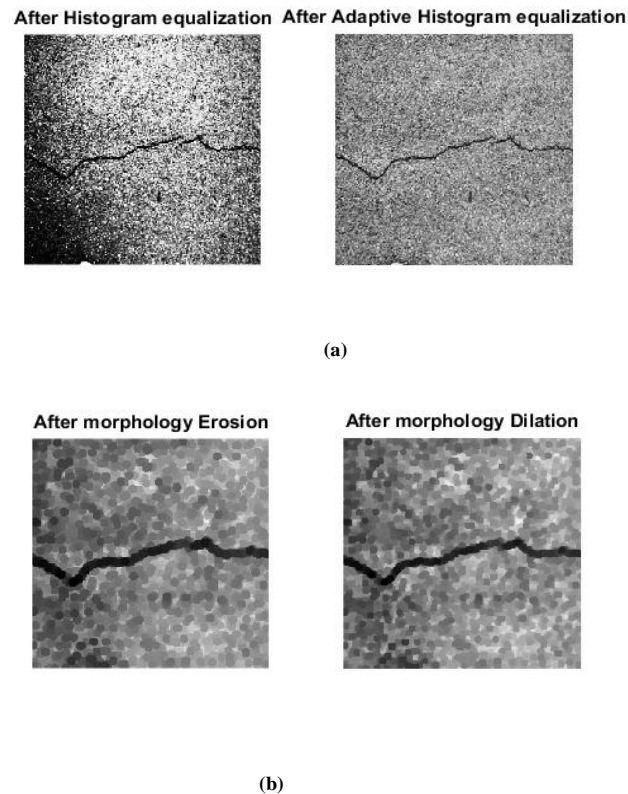


Fig. 13. GUI for Ancient Monument Crack Detection (a) Defective (b) non-Defective

Figure 13 depicts this in order to accomplish the aforementioned research goals, a user-friendly GUI was designed and built for automated crack detection.

Certainly, addressing potential challenges or limitations in accurately detecting and classifying cracks is crucial for providing a comprehensive evaluation of the proposed approach. Some potential limitations to consider include:

1. **Image Quality:** The effectiveness of crack detection may be impacted by variations in image quality, such as lighting conditions, resolution, and image artifacts. Poor-quality images may lead to inaccuracies in crack detection and classification.
2. **Complex Crack Patterns:** Ancient monuments often exhibit complex crack patterns, which may be challenging to accurately detect and classify. The proposed method may struggle to differentiate between cracks and natural features or surface irregularities, leading to false positives or false negatives.
3. **Generalization:** The performance of the proposed approach may vary across different types of ancient monuments or architectural styles. It may not generalize well to structures with unique characteristics or crack patterns that were not adequately represented in the training data.

5. Conclusion and Future Scope

In conclusion, this study introduces a novel approach for the detection of cracks in historic buildings, utilizing support vector machines (SVMs) and bias-parameter neural networks (BPNNs). Through the application of these machine learning algorithms, we have demonstrated their effectiveness in identifying and isolating damage depicted in photographs of historical structures. Our methodology involves the utilization of adaptive histogram equalization to enhance images of ancient monuments, followed by the extraction of features from these enhanced images. These features are then inputted into a classifier trained to distinguish between cracked and uncracked images of the ancient monument. The results of our research indicate that the proposed method, utilizing the AMCD III system, achieves high levels of sensitivity (97.37%), specificity (97.30%), and accuracy (97.33%). These findings underscore the potential of machine learning techniques in the field of heritage conservation, offering a reliable and efficient tool for assessing structural integrity and identifying areas of concern in historic buildings.

Looking ahead, future research endeavors may extend this investigation to encompass the detection of breaks in video frames, as well as the development of methods for identifying missing fasteners in historic buildings. Additionally, further improvements and refinements to the proposed approach could enhance its applicability and effectiveness in real-world conservation scenarios. Overall, this study represents a significant contribution to the field of heritage conservation, providing a robust and scalable solution for the detection of cracks in historic buildings. By leveraging machine learning techniques, we aim to support efforts to preserve and safeguard our cultural heritage for future generations.

References:

- [1] Kordatos, E.Z., Exarchos, D.A., Stavrakos, C., Moropoulou, A. and Matikas, T.E., "Infrared thermographic inspection of murals and characterization of degradation in historic monuments," *Construction and Building Materials*, 48, pp. 1261-1265, 2013.
- [2] Avdelidis, N. P. and Moropoulou, A., "Applications of infrared thermography for the investigation of historic structures," *Journal of Cultural Heritage*, 5(1), pp. 119- 127,2004
- [3] Moropoulou, A., Avdelidis, N.P., Kouli, M. and Kanellopoulos, N.K. , "Dual band infrared thermography as a NDT tool for the characterization of the building materials and conservation performance in historic structures," *MRS Online Proceedings Library Archive* ,591 ,1999.
- [4] Mérillou, S., and Ghazanfarpour, D., "A survey of aging and weathering Phenomena in computer graphics. *Computers&Graphics*," 32(2), pp.159-174, 2008.
- [5] Fitzner, B., Heinrichs, K., and Kownatzki, R., "Weathering forms at natural stone monuments: Classification, mapping and evaluation," *Internationale eitschrift für Bauinstandsetzen International journal for restoration of buildings and monuments*, 3(2), pp. 105- 124,1997
- [6] Schaffer, R. J., " The weathering of natural building stones," Routledge,2016
- [7] Fitzner, B. and Heinrichs, K., "Photo atlas of weathering forms on stone monuments," *Geological Institute, RWTH Aachen University–Working Group Natural stones and weathering*,2004
- [8] Ema, N.P., Alvarez de Buergo, M.A. And Rosa Bustamante, R., "Effects of conservation interventions on the archaeological Roman site of Merida (Spain). *Advance of research*," *Procedia Chemistry*, 8, pp. 269-278, 2013.
- [9] Alakkari, K. Abotaleb, M. Badr, A. Kadi, A. M., A. Mohamad, B. M., E. "Modelling Weather Conditions Using Encoder-Decoder and Attention Based on LSTM Deep Regression Model," *Journal of International Journal of Advances in Applied Computational Intelligence*, vol. 1, no. 2, pp. 08-29, 2022. **DOI:** <https://doi.org/10.54216/IJAACI.010201>
- [10] Price, C.A. and Doehne, E., "Stone conservation: an overview of current research", Getty publications, 2011.
- [11] Bandeira, D., and Walter, M., "Highlights on weathering effects," *The Visual Computer*, 26 (6-80), pp. 965-974,2010
- [12] Mérillou, S., and Ghazanfarpour, D., "A survey of aging and weathering phenomena in computer graphics ," *Computers & Graphics* , 32(2), pp. 159 -174, 2008
- [13] Verstrynge, E., Adriaens, R., Elsen, J. and Van Balen, K., "Multi-scale analysis on the influence of moisture on the mechanicbehavior of ferruginous sandstone," *Construction and Building Materials*, 54, pp. 78- 90, 2014.
- [14] Dong, J., Kim, B., Locquet, A., McKeon, P., Declercq, N. and Citrin, D.S., "Non-destructive evaluation of forced delamination in glass fiber- reinforced composites by terahertz and ultrasonic waves ," *Composites Part B: Engineering* ,79 , pp.667- 675,2015.
- [15] Péronnet, E., Eyma, F., Weleman, H. and Mistou, S.,"Characterization and comparison of defects detection limits of ultrasonic non destructive techniques," *Key Engineering Materials*, Vol. 498, pp. 79-88, Trans Tech Publications Ltd,2012.

- [16] Fais, S., Casula, G., Cuccuru, F., Ligas, P. and Bianchi, M.G. ,“An innovative methodology for the non-destructive diagnosis of architectural elements of ancient historical buildings,”*Scientific reports* 8(1), pp. 1-11, 2018
- [17] Ghoshal, A., Ayers, J., Gurvich, M., Urban, M. and Bordick, N., “Experimental investigations in embedded sensing of composite components in aerospace vehicles,” *Composites Part B: Engineering*, 71, pp. 52-62, 2015.
- [18] Kalpana, P., Anandan, R., Hussien, A.G. *et al.* Plant disease recognition using residual convolutional enlightened Swin transformer networks. *Sci Rep* **14**, 8660 (2024). <https://doi.org/10.1038/s41598-024-56393-8>.
- [19] Nappi, A. and Cote, P., “Nondestructive test methods applicable to historic stone structures,” *ENVIRONMENTAL SCIENCES RESEARCH REPORT ES*, 20, pp. 151- 166, 1997.
- [20] Kalpana, P., Anandan, R. (2023). A capsule attention network for plant disease classification. *Traitement du Signal*, Vol. 40, No. 5, pp. 2051-2062. <https://doi.org/10.18280/ts.400523>.
- [21] K., V. "Energy Aware Routing Protocol with Data Fusion and Machine Learning," *Journal of International Journal of Wireless and Ad Hoc Communication*, vol. 5, no. 1, pp. 22-35, 2022. **DOI:** <https://doi.org/10.54216/IJWAC.050102>
- [22] Mishra, M., Bhatia, A.S. and Maity, D.,“A comparative study of regression, neural network and neuro-fuzzy inference system for determining the compressive strength of brick– mortar masonry by fusing nondestructive testing data ,” *Engineering with Computers* , pp. 1-15,2019.
- [23] Pascale, G. and Lolli, A., “Crack assessment in marble sculptures using ultrasonic measurements: laboratory tests and application on the statue of David by Michelangelo,” *Journal of Cultural Heritage* 16(6), pp. 813-821, 2015.
- [24] Martinho, E., Dionísio, A., Almeida, F., Mendes, M. and Grangeia, C., “Integrated geophysical approach for stone decay diagnosis in cultural heritage,” *Construction and Building Materials*, 52, pp. 345-352, 2014.
- [25] Tavukcuoglu, A.Y.Ş.E. and Caner-Saltik, E.N., “Mapping of visual decay forms and infrared imaging of stone structures for the maintenance and monitoring studies,” 1999.
- [26] Salman, M., Mathavan, S., Kamal, K. and Rahman, M.,“ Pavement crack detection using the Gabor filter,” 16th international IEEE conference on intelligent transportation systems (ITSC), IEEE,2013
- [27] Moropoulou, A., Kouli, M., Theoulakis, P., Kourteli, C. and Zezza, F., “Digital Image processing for the environmental impact assessment on architectural surfaces,” *Journal of Environmental Chemistry and Technology*, 1, pp. 23-32, 1995.
- [28] Douglas-Jones, R., Hughes, J.J., Jones, S. and Yarrow, T., “Science, value and material decay in the conservation of historic environments,” *Journal of Cultural Heritage*, 21, pp.823-833, 2016.
- [29] Costamagna, E., Quintero, M.S., Bianchini, N., Mendes, N., Lourenço, P.B., Su, S., Paik, Y.M. and Min, A., “Advanced non-destructive techniques for the diagnosis of historic buildings: The Loka-Hteik-Pan temple in Bagan,” *Journal of Cultural Heritage*, 43, pp. 108-117, 2020.
- [30] Fitzner, B., “Damage diagnosis on stone monuments-in situ investigation and laboratory Studies,” *Proceedings of the International Symposium of the Conservation of the Bangudae Petroglyph*. Vol. 7, pp. 29-71, 2002.
- [31] Sýkora, M., Diamantidis, D., Holický, M., Marková, J. and Rózsás, Á. “Assessment of compressive strength of historic masonry using non-destructive and destructive techniques,” *Construction and Building Materials*, 193, pp. 196-210, 2018.
- [32] Mohan, A. and Poobal, S., “Crack detection using image processing: A critical review and analysis,” *Alexandria Engineering Journal*, 57(2), pp. 787-798, 2018.

- [33] Fort, R., de Buergo, M.A. and Perez-Monserrat, E.M., "Non-destructive testing for the assessment of granite decay in heritage structures compared to quarry stone," *International Journal of Rock Mechanics and Mining Sciences*, 61, pp.296-305,2013.
- [34] Brooks, A.J., Hussey, D.S., Yao, H., Haghshenas, A., Yuan, J., LaManna, J.M., Jacobson, D.L., Lowery, C.G., Kardjilov, N., Guo, S. and Khonsari, M.M., "Neutron interferometry detection of early crack formation caused by bending fatigue in additively manufactured SS316 dogbones," *Materials & Design*, 140, pp.420-430,2018.
- [35] Garnier, C., Pastor, M.L., Eyma, F. and Lorrain, B., "The detection of aeronautical defects in situ on composite structures using Non Destructive Testing," *Composite structures*, 93(5), pp. 1328-1336,2011.
- [36] Shehata, H.M., Mohamed, Y.S., Abdellatif, M. and Awad, T.H., (2018), "Depth estimation of steel cracks using laser and image processing techniques. *Alexandria engineering journal*," 57(4), pp.2713-2718.
- [37] Dare, P., Hanley, H., Fraser, C., Riedel, B. and Niemeier, W., (2002), "An operational application of automatic feature extraction: the measurement of cracks in concrete structures," *The Photogrammetric Record* 17(99), pp. 453-464.
- [38] Jung, H., Lee, C. and Park, G., (2017), "Fast and Non-invasive Surface Crack Detection of Press Panels Using Image Processing," *Procedia Engineering*, 188, pp. 72-79
- [39] Qingguo, T., Qijun, L., Ge, B. and Li, Y., (2019), "A methodology framework for retrieval of concrete surface crack's image properties based on hybrid model." *Optik*, 180, pp. 199-214.
- [40] Aslam, Y., Santhi, N., Ramasamy, N. and Ramar, K., (2020), "Localization and segmentation of metal cracks using deep learning," *Journal of Ambient Intelligence and Humanized Computing*, pp.1-9
- [41] Talab, A.M.A., Huang, Z., Xi, F. and HaiMing, L., (2016), "Detection crack in image using Otsu method and multiple filtering in image processing techniques," *Optik – Int. J. Light Electron* 127(3), pp.1030-1033.
- [42] Sankarasrinivasan, S., Balasubramanian, E., Karthik, K., Chandrasekar, U. and Gupta, R.,(2015), "Health monitoring of civil structures with integrated UAV and image processing system," *Procedia Computer Science*, *Procedia Computer Science*, 54, pp.508- 515
- [43] Turakhia, N., Shah, R., & Joshi, M. (2012, December). Automatic crack detection in heritage site images for image inpainting. In *Proceedings of the Eighth Indian Conference on Computer Vision, Graphics and Image Processing* (pp. 1-8).
- [44] Wicaksono, Y., Wahono, R.S. and Suhartono, V., (2015), "Color and texture feature extraction using gabor filter-local binary patterns for image segmentation with fuzzy C-means," *Journal of Intelligent Systems*,1(1), pp.15-21.
- [45] Ojala, T., Pietikainen, M. and Maenpaa, T., (2002), "Multiresolution gray-scale and rotation invariant texture Classification with local binary patterns," *IEEE Trans Pattern Anal Mach Intell*, 24(7), pp.971-987.
- [46] Akkoyun, O. and Toprak, Z.F., 2012, "Fuzzy-based quality classification model for natural building stone blocks," *Engineering geology*, 133, pp.66-75
- [47] Gonzalez Rafael, C. and Woods Richard, E., (2007), "Digital Image Processing," third Edition.
- [48] Al-Jubouri, Q., Al-Azawi, R.J., Al-Taei, M. and Young, I.,(2018), "Efficient individual identification of zebrafish using Hue/Saturation/Value color model," *The Egyptian Journal of Aquatic Research*, 44(4), pp.271-277
- [49] Jayaraman, E. and Esakkirajan, S., Veerakumar,(2010) "Digital Image Processing," Tata Mc Graw Hill. Education